High Resolution Fourier Transform Ion Cyclotron Resonance Mass Spectrometry (FT-ICR MS) for the characterisation of enzymatic processing of commercial lignin

Accepted Manuscript

Title: High Resolution Fourier Transform Ion Cyclotron Resonance Mass Spectrometry (FT-ICR MS) for the characterisation of enzymatic processing of commercial lignin

Authors: Virginia Echavarri-Bravo, Matthias Tinzl, Will Kew, Faye Cruickshank, C. Logan Mackay, David J. Clarke, Louise E. Horsfall

PII: S1871-6784(18)31920-4
DOI: https://doi.org/10.1016/j.nbt.2019.03.001
Reference: NBT 1168

To appear in:

Please cite this article as: Echavarri-Bravo V, Tinzl M, Kew W, Cruickshank F, Logan Mackay C, Clarke DJ, Horsfall LE, High Resolution Fourier Transform Ion Cyclotron Resonance Mass Spectrometry (FT-ICR MS) for the characterisation of enzymatic processing of commercial lignin, *New BIOTECHNOLOGY* (2019), https://doi.org/10.1016/j.nbt.2019.03.001

High Resolution Fourier Transform Ion Cyclotron Resonance Mass Spectrometry (FT-ICR MS) for the characterisation of enzymatic processing of commercial lignin.

Virginia Echavarri-Bravo[a], Matthias Tinzl[a], Will Kew[b], Faye Cruickshank[b], C. Logan Mackay[b], David J. Clarke[b]*, Louise E. Horsfall[a]*.

[a] School of Biological Sciences, Roger Land Building, University of Edinburgh, The King's Buildings, Alexander Crum Brown Road, Edinburgh, UK, EH9 3FF.

[b] EaStChem, School of Chemistry, The University of Edinburgh, David Brewster Road, Edinburgh, UK, EH9 3FJ.

* Corresponding authors
E-mail: Louise.Horsfall@ed.ac.uk.

Tel: +44 (0)131 650 5363

E-mail: dave.clarke@ed.ac.uk.

Tel: +44 (0)131 650 4808

Highlights

- FT-ICR MS allows changes in the chemical diversity of lignin to be monitored.
- A laccase from *T.versicolor* targeted sulfur-containing polymeric lignin species.
- Significant decrease in the number of assigned lignin compounds was detected.
- FT-ICR MS can aid the development and optimisation of laccase-mediator systems.

Abstract

Lignin and lignin components of woody biomass have been identified as an attractive alternative to fossil fuels. However, the complex composition of this plant polymer is one of the drawbacks that limits its exploitation. Biocatalysis of lignin to produce platform chemicals has been receiving great attention as it presents a sustainable approach for lignin valorisation. Aligned with this area of research, in the present study we have applied ultra-high-resolution Fourier transform ion cyclotron resonance mass spectrometry (FT-ICR MS)

to identify the preferred lignin substrates of a ligninolytic enzyme, a laccase produced by the terrestrial fungus *Trametes versicolor*. A commercial lignin was incubated with the laccase and acetosyringone (a laccase mediator) for up to 168h and direct infusion electrospray FT-ICR MS enabled the identification of thousands of molecular species present in the complex lignin sample at different incubation time points. Significant changes in the chemical composition of lignin were detected upon laccase treatment, which resulted in a decrease in the molecular mass distribution of assigned species, consistent with laccase lytic activity. This reduction was predominantly in species classified as lignin-like (based on elemental ratios) and polymeric in nature (>400 Da). Of particular note was a fall in the number of species assigned containing sulfur. Changes in the chemical composition/structure of the lignin polymer were supported by FT-IR spectroscopy. We propose the use of FT-ICR MS as a rapid and efficient technique to support the biotechnological valorisation of lignin as well as the development and optimization of laccase-mediator systems for treating complex mixtures.

List of abbreviations

FT-ICR MS: Fourier transform ion cyclotron resonance mass spectrometry

FTIR: Fourier-transform infrared spectroscopy

LMS: Laccase-mediator system

ET: Electron Transfer

HAT: Hydrogen Atom Transfer

ABTS: 2,2'-azino-bis(3-ethylbenzothiazoline-6-sulphonic acid)

HBT: 1-hydroxybenzotriazole

HPLC/MS: High-performance liquid chromatography/mass spectrometry

DMSO: Dimethyl sulfoxide

SORI-CID: Sustained off-resonance irradiation collision-induced dissociation

Keywords

FT-ICR MS, laccase, lignin, complex mixture, acetosyringone

Introduction

Lignin is one of the three major components of the cellular wall in vascular plants [1] and can constitute up to 30% by dry weight in the wood of conifers [2]. Its main functions consist of conferring structural rigidity and permeability to the plant, as well as playing a major role as a protective barrier against microbial infection. The lignin polymer is composed of phenylpropanoids, principally three hydroxycinnamyl alcohols, coniferyl, sinapyl and ρ-coumaril, which are also known as monolignols. These units are connected by different linkages, the presence and relative abundance of which differ across plant groups, with the β–O-4' linkage being the most abundant (45-50% softwood, 60% hardwood) followed by 5-5' (3-22%), β-5 (3-12%), β–β (2- 12%), β-1 (1-9%) and 4-O-5 (4-9%) [3]. The high abundance of this plant polymer makes lignin one of the most promising sources of platform chemicals (e.g. aromatic building blocks)[4], potentially capable of replacing fossil fuels [3]. However, lignin molecules are highly complex and recalcitrant to decomposition. Hence, the use of lignin for the production of high value molecules is still underexploited; in the bioethanol and paper industries, where most of the lignin is generated, it is generally burned for the production of thermal energy [5]. However, this practice may change rapidly during the next few years as a result of circumstances such as restrictions in CO_2 emission levels due to climate change and the depletion of fossil fuels. Moreover, the broad range of applications and technologies obtained from lignin-derived products (e.g. concrete additives, industrial binders, and biopolymers for ceramics) has been demonstrated by a few pioneering companies [6–8], and shows that the valorisation of lignin by conversion into bio-based compounds can be a more profitable alternative than incineration. Numerous depolymerisation routes have been investigated to date [9], with enzymatic breakdown being one of the most environmentally benign (greenest) alternatives as it has low energy requirements (reactions are conducted at the relatively low temperature of 20-30°C) and does not involve the use of toxic chemicals or solvents.

Laccases (benzenediol:oxygen oxidoreductases, EC 1.10.3.2) are enzymes produced by a wide range of organisms, including plants, insects, fungi, archaea and bacteria. Bacterial and fungal laccases are used as biocatalysts in diverse industries due to their ability to oxidise a wide range of phenolic and other aromatic substrates; examples are break down of textile dyes [10] and other micropollutants [11] , functionalisation of wood fibres for the production of composite boards free from formaldehyde-based adhesives [12] and potential applications towards the development of a sustainable refining industry for biomass pre-treatment, lignin valorisation and the detoxification of waste streams [13]. Due to their relatively low redox potential, laccases require the presence of small molecules known as mediators to oxidise non-phenolic compounds such as α–hydroxyl groups and to

cleave β-O-4-ether bonds [13]. Several molecules have been identified for use in a laccase-mediator system (LMS) to enable the oxidation of a wider range of inorganic and organic compounds including lignin [14]. These mediators couple the oxidation of the substrate through two different mechanisms, the Electron Transfer (ET) system or the radical Hydrogen Atom Transfer (HAT) route. Two of the most extensively used mediators for the LMS are 2,2'-azino-bis(3-ethylbenzothiazoline-6-sulphonic acid) (ABTS) and 1-hydroxybenzotriazole (HBT), [13,15–18] which react with laccase substrates via the ET and HAT routes respectively [17].

The aim of the present study was to assess the applicability of ultra-high-resolution mass spectrometry (Electrospray Ionisation Fourier transform ion cyclotron resonance mass spectrometry (ESI FT-ICR MS)) to investigate effects of a laccase on lignin and to determine the substrate specificity of this enzyme. The high mass accuracy and mass resolution of FT-ICR MS enables the elemental assignment of thousands of compounds present in complex mixtures such as lignin [19–22] and bio-oils from lignocellulosic material [23–25]. In this study, a commercial lignin product was incubated with laccase produced by the terrestrial fungus *T. versicolor* [26], well known for producing ligninolytic enzymes [27,28], together with the natural mediator acetosyringone [29]. FT-ICR MS was used to monitor chemical changes accompanying enzyme-treatment. The potential of using FT-ICR MS for the analysis of products derived from lignin model compounds after treatment with laccase has recently been highlighted [15]. However, as far as we are aware, this study is the first in which FT-ICR MS has been used to characterise changes in the chemical composition of a complex mixture such a commercial lignin upon enzymatic treatment.

Materials and Methods

Reagents

Kraft lignin (471003, low sulfonate content; 4% total sulfur content – determined by supplier), laccase from *T. versicolor* (code 51639), Acetosyringone (D1344063′,5′-Dimethoxy-4′-hydroxyacetophenone) and 2,2′-Azino-bis (3-ethylbenzothiazoline-6-sulfonic acid) diammonium salt (ABTS) were from Sigma-Aldrich (St. Louis, MO). High-performance liquid chromatography/mass spectrometry (HPLC/MS) grade water and dimethyl sulfoxide (DMSO) were from Fisher Scientific (Pittsburgh, PA). All chemicals were used without further purification.

Incubation of kraft lignin with laccase

The incubation of kraft lignin with laccase was performed in 100 ml glass conical flasks at 25°C and 200 rpm in an orbital shaker to enhance oxygenation. The medium composition consisted of ammonium acetate buffer (20mM,pH 4.5), laccase from *T.*

versicolor (51639) 25 µg ml^{-1} (enzyme activity 200U measured with ABTS substrate), acetosyringone dissolved in (DMSO) (0.2 mM) and kraft lignin (5 mg ml^{-1} FT-IR spectroscopy, 2 mg ml^{-1} FT-ICR MS). This lignin product is completely soluble in water at 25°C and at the concentrations used [30] due to the presence of sulfonate/sulfonic groups [31]. For FT IR analysis, incubation was for 168h and 6 experimental replicates were performed. In addition, two negative controls were introduced, (i) lignin only (no mediator, no laccase), and (ii) lignin with mediator (no laccase). For FT-ICR MS analysis, the incubation of laccase with the mediator was carried out in triplicate. Negative controls, without laccase, were prepared similarly. Sample aliquots (0.5 ml) were collected at several time points (0, 0.5, 2, 24, 72,and168h), mixed with and equal volume of 100% methanol (ratio 1:1) to quench the reaction [32] and stored at 4°C.

Fourier-transform infrared (FT IR) spectroscopy

For FT IR analysis, samples were freeze-dried after incubation for 168h and FT IR spectra were registered using a PerkinElmer Spectrum 65 spectrometer with a Pike Technologies diamond MIRacle ATR device. The spectra were collected from 4000 to 600 cm^{-1} with 32 scans and 4 cm^{-1} resolution. ATR correction and normalisation of spectra to 50% transmittance at 1502 cm^{-1} was performed using the PerkinElmer software. For each sample three independent measurements were taken. Absorbance data was normalised for principal component analysis (PCA) as described elsewhere[33].

ESI (-) FT-ICR Mass Spectrometry

Prior to FT-ICR MS analysis samples were diluted in 1:1 methanol and water to a final concentration of 100-200 µg ml^{-1}. Mass spectra were acquired by direct infusion on a 12 Tesla SolariX FT-ICR MS (Bruker Daltonics, Billerica, Massachusetts, USA) using an electrospray ionisation ESI source. Nebuliser gas flow was set to 1.8 bar, drying gas was 6 L/min at 180°C. Typically, broadband spectra were acquired with 100 summed scans between 98.3 *m/z* and 1000 *m/z* into a 4 MW FID of 1.1185 s. Time of flight was set to 0.6 ms with an ion accumulation time of 150 ms. Three technical replicates were analysed per treatment to validate instrument reproducibility. To minimise any carryover effects between samples, the syringe, capillary and sprayer were thoroughly flushed between samples with methanol:water. Spectra were acquired in negative-ion mode, as the preference for negative mode ESI (-) analysis of complex mixtures has been widely reported elsewhere [34–40]. For isotopic fine structure analysis, continuous accumulation of selected ions (CASI) was employed with the quadrupole width set to 20 *m/z*, and an ion accumulation time of 2000 ms. For tandem mass spectrometry, individual species were fragmented using sustained off-resonance irradiation collision-induced dissociation (SORI-CID). Signal intensity was increased using CASI (with a quadrupole window of 10 *m/z*) and the ion accumulation time

was increased to 20-60 seconds. Fragmentation was induced with SORI-CID (using pulsed nitrogen and frequency offset of 500 Hz). SORI power was varied to achieve maximum fragmentation (typically 0.5-0.8%).

Data analysis

The collected spectra were calibrated and the list of peaks generated in Data Analysis 4.4 (Bruker Daltonics) as described elsewhere [39]. The calibration list depicted in Table S1 was configured based on a number of compounds identified in the literature and with elemental assignments validated in this work. Formula assignment was performed by PetroOrg S-10.2 (Florida State University, Tallahassee, USA) with the elemental limits $C_{1\text{-}100}$ $H_{1\text{-}200}$ $O_{1\text{-}30}$ $S_{0\text{-}2}$ and with a maximum error threshold of 500 ppb. Only singly-charged deprotonated species molecular ions were considered in the assignment of peaks. Van Krevelen plots were produced using in-house Python scripts and Matplotlib [40,41]; each assigned monoisotopic formula was represented as a circle on a scatter graph based on the O/C ratio versus H/C ratio. The circles were sized according to normalized relative peak intensity, where the sum of intensities per spectrum is set to 1. The circles were coloured according to mass.

Results and Discussion

FT IR spectroscopy

FT IR spectroscopy provides information about the presence of specific molecules and chemical bonds and has been extensively used to characterise the chemical structure of lignin [42–44]. Furthermore, this technique has been widely applied for monitoring changes in lignin with diverse treatments, such as biocatalytic [45], pyrolytic [46] and chemical [47] and it was used here to investigate the effects of the laccase on a commercial lignin product. Lignin was incubated with the laccase and the mediator acetosyringone for 168h before FT IR analysis. Relevant absorbance peaks in the IR spectra of different samples of lignin were identified (**Table 1**). No dramatic changes (e.g. disappearance/ appearance of new peaks) were observed upon initial inspection of the spectra. However, small differences in the region between 1700-1600 cm^{-1} were noted (**Figure 1**). A significant increase in absorbance was detected in the samples treated with the laccase within this region, which is diagnostic for the carbonyl bond.

The PCA of the absorbance at selected wavelengths showed a clear shift of the samples after laccase treatment (n=6) towards the positive X-axis and the negative Y-axis (Figure 1). The principal components PC1 and PC2 described up to 68.87% of the total variability between samples. Major changes were associated with wavelengths 1700 and 1591 cm^{-1}, both corresponding to carbonyl bonds; details of the PC1 and PC2 loadings are

given in **Table 2**. Higher presence of carbonyl bonds after incubation with laccase suggests a higher oxidation state of the lignin polymer. The oxidation of primary alcohols resulting in carboxylic or/and aldehydes groups, as well as in ketone groups from secondary alcohols, has been reported in previous reports using laccases from *T. versicolor* and different mediators such as TEMPO [48] and 1-HBT [15,49]. The samples in the control treatments (lignin alone (n=2) and the negative control (n=2)) did not show clear changes after 168h incubation.

ESI FT-ICR-MS analysis of lignin allows the assignment of thousands of elemental formulae and highlights the chemical complexity of commercial lignin.

The utility of FT-ICR MS for fingerprinting lignin and lignin-derived samples has recently been demonstrated [19–21,50] as well as the identification of lignin molecules in a wide range of samples such as bio-oils [24], whisky [39,40,51] and drinking water [52]. In addition, the technique shows great promise for the characterisation of changes in the chemical diversity of complex biological samples [53]. The enzymatic treatment was allowed to progress for 168h and samples were collected at time points throughout the incubation. 42 samples were analysed in total, including experimental and technical replicates for the laccase treatment and the negative control at different incubation time points. Initial analysis of technical replicates confirmed the reproducibility of the analysis (data not shown); and experimental replicates were used in all subsequent data analyses.

The representative mass spectrum of one of the samples collected from the laccase treatment at time 0h is depicted in **Figure 2**. The acquired mass spectrum consisted of over 3350 peaks (S/N>4), with mass resolution of ~300,000 at *m/z* 400, highlighting the high chemical complexity of the sample. After data acquisition, internal calibration was performed using a calibration list prepared in-house from 55 compounds known to be present in lignin (Table S1). The high mass accuracy and resolving power of FT-ICR MS enables the determination of elemental formulae directly from mass measurement. This is exemplified in Figure 2B where 11 peaks within a single nominal *m/z* (*m/z* 355) were unambiguously assigned a molecular formula with mass errors of approximately 100 ppb (**Table 3**). Using in-house scripts and commercial software, elemental formula assignments were made for each spectrum obtained. Although formulae were first assigned based on CHO elemental composition, initial analysis revealed that over half the assigned species contained sulfur (CHOS species). In total, over all 42 datasets, 3137 different elemental formulae were assigned and in each individual dataset, the total number of elemental formula assignments varied between 1152 and 1742.

In order to confirm the assignments of sulfur containing species in the kraft lignin samples, isotope fine structure (IFS) analysis was performed on several CHOS species.

Particular attention was paid to the isotopic fine structure of the [M+2] isotope where mass defect difference between $^{13}C_2$, ^{18}O and ^{34}S is most apparent. In all examples analysed, IFS analysis confirmed original assignments (Figure S1).

The global assignment of elemental formula allows the visualisation of each dataset as Van Krevelen (VK) diagrams [55] based on the O/C and H/C ratios (Figure 2C). In addition, the chemical species could be classified into four major groups based on their assigned elemental composition and elemental ratios: lignin O/C:0.3-0.7 and H/C: 1-1.5; condensed aromatics O/C <0.25 and H/C: 0.5-1.0; fatty acids or esters/lipids O/C <0.2 and H/C: 1.6-2.0; carbohydrates O/C: 0.8 – 1.0 and H/C: 1.65 – 2.0 [55,56]. The percentage of each group (based on the number of compounds assigned) is depicted in Figure 2D. As expected, the peaks associated with lignin-type species are the most abundant, up to 48.7% of the total compounds assigned fall into this group based on the O/C and H/C ratios.

ESI FT-ICR-MS revealed chemical changes in commercial lignin after laccase treatment.

In order to investigate the chemical changes associated with laccase processing of lignin, the changes in the elemental assignments over time were compared. On initial inspection, it was apparent that the total number of chemical species decreased significantly by 23% (RM ANOVA $p<0.001$), during the first 0.5h of incubation with laccase and continued to decrease over 24h (**Figure 3**A). A similar trend was observed with the abundance of peaks classified as lignin which also reduced significantly (25%) (Figure 3B). In contrast, no significant change was observed in the number of peaks assigned in the negative controls. As noted above, a large proportion of the elemental formulae assigned in the lignin substrate contained sulfur. The analysis highlighted that the number of these S-containing species decreased over 24h (**Figure 4**A). In particular, sulfur containing lignin species where dramatically reduced upon laccase treatment with 46% reduction in S-containing assignments after 24h incubation (Figure 4B).

This change can be visualised by VK diagrams for lignin samples before and after laccase treatment (**Figure 5**); these plots display a clear reduction in the density of species within the lignin region after enzyme treatment (O/C:0.3-0.7 and H/C: 1-1.5). From the datasets, a subset of species was defined, the disappearance of which was associated with laccase treatment. In order to do this, the data was filtered to include assigned species according to the following criteria:

(i) species were present in all technical and experimental replicates in both treatments (laccase, negative control) at 0h.
(ii) species were not present in all samples incubated with laccase after 168h
(iii) species were present in all samples from the negative control after 168h.

This resulted in a subset of 169 assignments (Table S2). By visualising these species on a VK diagram it is clear that the majority fall in the lignin-region (O/C:0.3-0.7 and H/C: 1-1.5) (Figure S2). Surprisingly we also noted that 66.9% of these were CHSO species, suggesting that sulfur-containing lignin type species are favoured substrates for the laccase.

The molecular mass distribution was analysed of the species assigned in the lignin samples before and after laccase-acetosyringone treatment. Frequency distributions were constructed for the *m/z* range which corresponds to monomeric (<250 Da), dimeric (250-400 Da) and higher order (400-500 Da and >500 Da) lignin-based molecules [19,57] (**Figure 6**). The analysis highlighted that the reduction of assignments associated with laccase treatment was predominantly in larger lignin-type species – the number of species assigned in the mass ranges 400-500 Da and >500 Da fell from 279 to 166 and from 170 to 25 respectively. In contrast the monomeric and dimeric species were largely unaffected by enzymatic treatment; indeed, a small increase (70 to 77) was observed in species of mass <250 Da. This observation suggests that the laccase activity was predominantly lytic in nature – i.e. catalysing the cleavage of polymeric lignins into smaller species. Further analysis of the frequency distribution of heteroatomic classes highlights the dramatic reduction in sulfur-containing assignments in polymeric lignin species (Figure S3a-d).

Characterisation of sulfur containing species by tandem mass spectrometry.

Finally, in order to investigate the chemical nature of the sulfur in the CHOS assignments, tandem MS experiments were performed. Briefly, the monoisotopic peaks of specific species assigned as CHOS were isolated and fragmented using a combination of CASI and SORI-CID. Four sulfur-containing assignments were chosen from the O_9S class ($C_{20}H_{24}O_9S$, $C_{21}H_{24}O_9S$, $C_{21}H_{26}O_9S$ and $C_{21}H_{28}O_9S$). The relative abundance of the first three decreased on treatment with laccase, and the peak for $C_{21}H_{28}O_9S$ disappeared. In all species analysed, fragments consistent with the loss of SO_3H_2 were observed, and in addition loss of both CH_2 and CH_2O was common (**Table 4**). These findings suggest that the sulfur is commonly present as sulfonate/sulfonic acid groups in CHOS compounds in lignin. This is in agreement with a recent study of *T. versicolor,* the source of the laccase in this work, which demonstrated that sulfonate was a preferred source of sulfur when grown on wood biomass [58]. In agreement with previous work [59], we propose that the desulfonation occurs *via* destabilisation of the C-SO_3^- bond by an oxidation reaction catalysed by the laccase, and subsequent loss of the sulfonate.

Conclusion

We have shown that ESI (-) FT-ICR-MS is a rapid and efficient technique to monitor the effects of laccase on mixtures as complex as commercial lignin. By employing this strategy, it was possible to propose preferred substrates of *T. versicolor* laccase. FT-ICR-MS could be a key technique for the valorisation of lignin via enzymatic processes, affording a large amount of information from a single measurement: mass distributions and chemical sample composition, as well as allowing the identification of species which disappear upon lignin treatment and their sum formulae. The great potential of FT-ICR MS for the development and optimization of laccase-mediator systems shown here will find applications in diverse sectors, e.g. the paper industry for the development of biomass pre-treatment and pulp bleaching processes, the polymer industry for the production of bio-based polymers, and for optimizing processes for bioremediation of waste streams.

Author contributions

Louise Horsfall, David Clarke, Matthias Tinzl and Virginia Echavarri designed the experiments and formulated conclusions, Louise Horsfall and David Clarke supervised the work. Matthias Tinzl and Virginia Echavarri conducted the experiments and David Clarke, Faye Cruickshank, Will Kew and Logan Mackay helped with the FT-ICR MS data collection and analysis. Virginia Echavarri and David Clarke wrote the manuscript.

Conflict of interest

None declared.

Datasets

All mass spectrometry datasets used in this study are available to download, in their original data formats, from the Clarke Research Group repository at Edinburgh DataShare (www.http://datashare.is.ed.ac.uk/handle/10283/760), using the following link: http://hdl.handle.net/10283/3205.

Funding

This project was funded by IBioIC and an EPSRC Impact Acceleration Account (IAA) [FEAS-2016-1].

Acknowledgments

We wish to thank the Swiss European Mobility Programme (SEMP) for funding MT.

References

[1] Lynd LR, Weimer PJ, van Zyl WH, Pretorius IS. Microbial Cellulose Utilization: Fundamentals and Biotechnology. Microbiol Mol Biol Rev 2002;66:739–739. doi:10.1128/MMBR.66.4.739.2002.

[2] McKendry P. Energy production from biomass (part 1): overview of biomass. Bioresour Technol 2002;83:37–46. doi:10.1016/S0960-8524(01)00118-3.

[3] Zakzeski J, Bruijnincx PCA, Jongerius AL, Weckhuysen BM. The Catalytic Valorization of Lignin for the Production of Renewable Chemicals 2010:3552–99.

[4] Pellis A, Cantone S, Ebert C, Gardossi L. Evolving biocatalysis to meet bioeconomy challenges and opportunities. N Biotechnol 2018;40:154–69. doi:10.1016/J.NBT.2017.07.005.

[5] Fava F, Totaro G, Diels L, Reis M, Duarte J, Carioca OB, et al. Biowaste biorefinery in Europe: opportunities and research & development needs. N Biotechnol 2015;32:100–8. doi:10.1016/J.NBT.2013.11.003.

[6] Lignotech n.d. https://www.lignotech.com/ (accessed November 8, 2018).

[7] KTM Polymers n.d. http://www.kmtpolymers.com/ (accessed November 8, 2018).

[8] Rayonier n.d. https://rayonieram.com/ (accessed November 8, 2018).

[9] Sun Z, Fridrich B, De Santi A, Elangovan S, Barta K. Bright Side of Lignin Depolymerization: Toward New Platform Chemicals. Chem Rev 2018. doi:10.1021/acs.chemrev.7b00588.

[10] Abadulla E, Tzanov T, Costa S, Robra K-H, Cavaco-Paulo A, Gübitz GM. Decolorization and Detoxification of Textile Dyes with a Laccase from Trametes hirsuta. Appl Environ Microbiol 2000;66:3357 LP-3362.

[11] Margot J, Maillard J, Rossi L, Barry DA, Holliger C. Influence of treatment conditions on the oxidation of micropollutants by Trametes versicolor laccase. N Biotechnol 2013;30:803–13. doi:10.1016/J.NBT.2013.06.004.

[12] Widsten P, Kandelbauer A. Adhesion improvement of lignocellulosic products by enzymatic pre-treatment. Biotechnol Adv 2008;26:379–86. doi:https://doi.org/10.1016/j.biotechadv.2008.04.003.

[13] Roth S, Spiess AC. Laccases for biorefinery applications: a critical review on challenges and perspectives. Bioprocess Biosyst Eng 2015. doi:10.1007/s00449-015-1475-7.

[14] Morozova O V, Shumakovich GP, Shleev S V, Yaropolov YI. Laccase-mediator systems and their applications: A review. Appl Biochem Microbiol 2007;43:523–35. doi:10.1134/S0003683807050055.

[15] Hilgers R, Vincken JP, Gruppen H, Kabel MA. Laccase/Mediator Systems: Their Reactivity toward Phenolic Lignin Structures. ACS Sustain Chem Eng 2018. doi:10.1021/acssuschemeng.7b03451.

[16] Johannes C, Majcherczyk A. Natural mediators in the oxidation of polycyclic aromatic hydrocarbons by laccase mediator systems. Appl Environ Microbiol 2000. doi:10.1128/AEM.66.2.524-528.2000.

[17] Munk L, Punt AM, Kabel MA, Meyer AS. Laccase catalyzed grafting of-N-OH type mediators to lignin via radical-radical coupling. RSC Adv 2017. doi:10.1039/c6ra26106j.

[18] Furukawa T, Bello FO, Horsfall L. Microbial enzyme systems for lignin degradation and their transcriptional regulation. Front Biol (Beijing) 2014. doi:10.1007/s11515-014-1336-9.

[19] Jarrell TM, Marcum CL, Sheng H, Owen BC, O'Lenick CJ, Maraun H, et al. Characterization of organosolv switchgrass lignin by using high performance liquid chromatography/high resolution tandem mass spectrometry using hydroxide-doped negative-ion mode electrospray ionization. Green Chem 2014;16:2713–27. doi:10.1039/c3gc42355g.

[20] D'Auria M, Emanuele L, Racioppi R. FT-ICR-MS analysis of lignin. Nat Prod Res 2012. doi:10.1080/14786419.2011.586947.

[21] Chatterjee S, Clingenpeel A, McKenna A, Rios O, Johs A. Synthesis and characterization of lignin-based carbon materials with tunable microstructure. RSC Adv 2014;4:4743–53. doi:10.1039/C3RA46928J.

[22] Qi Y, Volmer DA. Rapid mass spectral fingerprinting of complex mixtures of decomposed lignin: Data-processing methods for high-resolution full-scan mass spectra. Rapid Commun Mass Spectrom 2018. doi:10.1002/rcm.8254.

[23] Hertzog J, Carre V, Brech Y Le, Dufour A. Toward Controlled Ionization Conditions for ESI-FT-ICR-MS Analysis of Bio-Oils from Lignocellulosic Material 2016. doi:10.1021/acs.energyfuels.6b00655.

[24] Tessarolo NS, Silva RVS, Vanini G, Casilli A, Ximenes VL, Mendes FL, et al. Characterization of thermal and catalytic pyrolysis bio-oils by high-resolution techniques: 1H NMR, GC x GC-TOFMS and FT-ICR MS. J Anal Appl Pyrolysis 2016;117:257–67. doi:10.1016/j.jaap.2015.11.007.

[25] Miettinen I, Mäkinen M, Vilppo T, Jänis J. Compositional Characterization of Phase-Separated Pine Wood Slow Pyrolysis Oil by Negative-Ion Electrospray Ionization Fourier Transform Ion Cyclotron Resonance Mass Spectrometry. Energy & Fuels 2015;29:1758–65. doi:10.1021/ef5025966.

[26] Saraiva JA, Tavares APM, Xavier AMRB. Effect of the Inducers Veratryl Alcohol, Xylidine, and Ligninosulphonates on Activity and Thermal Stability and Inactivation Kinetics of Laccase from Trametes versicolor. Appl Biochem Biotechnol 2012;167:685–93. doi:10.1007/s12010-012-9719-3.

[27] Bourbonnais R, Paice MG, Reid ID, Lanthier P, Yaguchi M. Lignin oxidation by laccase isozymes from Trametes versicolor and role of the mediator 2,2'-azinobis(3-ethylbenzthiazoline-6-sulfonate) in kraft lignin depolymerization. Appl Environ Microbiol 1995.

[28] Jönsson LJ, Palmqvist E, Nilvebrant NO, Hahn-Hägerdal B. Detoxification of wood hydrolysates with laccase and peroxidase from the white-rot fungus Trametes versicolor. Appl Microbiol Biotechnol 1998. doi:10.1007/s002530051233.

[29] Camarero S, Ibarra D, Martínez MJ, Martínez ÁT. Lignin-derived compounds as efficient laccase mediators for decolorization of different types of recalcitrant dyes. Appl Environ Microbiol 2005. doi:10.1128/AEM.71.4.1775-1784.2005.

[30] Ma R, Hao W, Ma X, Tian Y, Li Y. Catalytic ethanolysis of kraft lignin into high-value small-molecular chemicals over a nanostructured α-molybdenum carbide catalyst. Angew Chemie - Int Ed 2014. doi:10.1002/anie.201402752.

[31] Ahvazi B, Cloutier É, Wojciechowicz O, Ngo TD. Lignin Profiling: A Guide for Selecting Appropriate Lignins as Precursors in Biomaterials Development. ACS Sustain Chem Eng 2016;4:5090–105. doi:10.1021/acssuschemeng.6b00873.

[32] Lu J, Shao J, Liu H, Wang Z, Huang Q. Formation of Halogenated Polyaromatic Compounds by Laccase Catalyzed Transformation of Halophenols. Environ Sci Technol 2015;49:8550–7. doi:10.1021/acs.est.5b02399.

[33] Virk AP, Puri M, Gupta V, Capalash N, Sharma P. Combined Enzymatic and Physical Deinking Methodology for Efficient Eco-Friendly Recycling of Old Newsprint. PLoS One 2013;8. doi:10.1371/journal.pone.0072346.

[34] Cooper HJ, Marshall AG. Electrospray Ionization Fourier Transform Mass Spectrometric Analysis of Wine. J Agric Food Chem 2001;49:5710–8. doi:10.1021/jf0108516.

[35] Møller JKS, Catharino RR, Eberlin MN. Electrospray ionization mass spectrometry fingerprinting of whisky: immediate proof of origin and authenticity. Analyst 2005;130:890. doi:10.1039/b415422c.

[36] Garcia JS, Vaz BG, Corilo YE, Ramires CF, Saraiva SASA, Sanvido GB, et al. Whisky analysis by electrospray ionization-Fourier transform mass spectrometry. Food Res Int 2013;51:98–106. doi:10.1016/j.foodres.2012.11.027.

[37] Roullier-Gall C, Witting M, Gougeon RD, Schmitt-Kopplin P. High precision mass measurements for wine metabolomics. Front Chem 2014. doi:10.3389/fchem.2014.00102.

[38] Sivalingam GN, Yan J, Sahota H, Thalassinos K. Amphitrite: A program for processing travelling wave ion mobility mass spectrometry data. Int J Mass Spectrom 2013;345–347:54–62. doi:10.1016/j.ijms.2012.09.005.

[39] Kew W, Goodall I, Clarke D, Uhrín D. Chemical Diversity and Complexity of Scotch Whisky as Revealed by High-Resolution Mass Spectrometry. J Am Soc Mass Spectrom 2017. doi:10.1007/s13361-016-1513-y.

[40] Kew W, Mackay CL, Goodall I, Clarke DJ, Uhrín D. Complementary Ionization Techniques for the Analysis of Scotch Whisky by High Resolution Mass Spectrometry. Anal Chem 2018. doi:10.1021/acs.analchem.8b01446.

[41] Kew W, Blackburn JWT, Clarke DJ, Uhrín D. Interactive van Krevelen diagrams – Advanced visualisation of mass spectrometry data of complex mixtures. Rapid Commun Mass Spectrom 2017. doi:10.1002/rcm.7823.

[42] Ahvazi B, Cloutier É, Wojciechowicz O, Ngo T-D. Lignin Profiling: A Guide for Selecting Appropriate Lignins as Precursors in Biomaterials Development. ACS Sustain Chem Eng 2016;4:5090–105. doi:10.1021/acssuschemeng.6b00873.

[43] Schwanninger M, Rodrigues JC, Pereira H, Hinterstoisser B. Effects of short-time vibratory ball milling on the shape of FT-IR spectra of wood and cellulose. Vib Spectrosc 2004;36:23–40. doi:10.1016/j.vibspec.2004.02.003.

[44] Boeriu CG, Bravo D, Gosselink RJA, Van Dam JEG. Characterisation of structure-dependent functional properties of lignin with infrared spectroscopy. Ind. Crops Prod., vol. 20, 2004, p. 205–18. doi:10.1016/j.indcrop.2004.04.022.

[45] Kumar M, Singh J, Singh MK, Singhal A, Thakur IS. Investigating the degradation process of kraft lignin by β -proteobacterium , Pandoraea sp . ISTKB 2015. doi:10.1007/s11356-015-4771-5.

[46] Han T, Sophonrat N, Evangelopoulos P, Persson H, Yang W, Jönsson P. Evolution of sulfur during fast pyrolysis of sulfonated Kraft lignin. J Anal Appl Pyrolysis 2018. doi:10.1016/j.jaap.2018.04.006.

[47] You T, Zhang L, Guo S, Shao L, Xu F. Unraveling the Structural Modifications in Lignin of Arundo donax Linn. during Acid-Enhanced Ionic Liquid Pretreatment. J Agric Food Chem 2015. doi:10.1021/acs.jafc.5b04831.

[48] Galletti P, Pori M, Funiciello F, Soldati R, Ballardini A, Giacomini D. Laccase-Mediator System for Alcohol Oxidation to Carbonyls or Carboxylic Acids: Toward a Sustainable Synthesis of Profens. ChemSusChem 2014. doi:10.1002/cssc.201402136.

[49] Heap L, Green A, Brown D, Van Dongen B, Turner N. Role of laccase as an enzymatic pretreatment method to improve lignocellulosic saccharification. Catal Sci Technol 2014. doi:10.1039/c4cy00046c.

[50] Qi Y, Hempelmann R, Volmer DA. Two-dimensional mass defect matrix plots for mapping genealogical links in mixtures of lignin depolymerisation products. Anal Bioanal Chem 2016;408:4835–43. doi:10.1007/s00216-016-9598-5.

[51] Roullier-Gall C, Signoret J, Hemmler D, Witting MA, Kanawati B, Schäfer B, et al. Usage of FT-ICR-MS Metabolomics for Characterizing the Chemical Signatures of Barrel-Aged Whisky. Front Chem 2018. doi:10.3389/fchem.2018.00029.

[52] Zhang H, Zhang Y, Shi Q, Ren S, Yu J, Ji F, et al. Characterization of low molecular weight dissolved natural organic matter along the treatment trait of a waterworks using Fourier transform ion cyclotron resonance mass spectrometry. Water Res 2012;46:5197–204. doi:10.1016/J.WATRES.2012.07.004.

[53] Yuan Z, He C, Shi Q, Xu C, Li Z, Wang C, et al. Molecular Insights into the Transformation of Dissolved Organic Matter in Landfill Leachate Concentrate during Biodegradation and Coagulation Processes Using ESI FT-ICR MS. Environ Sci Technol 2017. doi:10.1021/acs.est.7b02194.

[54] Kujawinski EB. Electrospray ionization Fourier transform ion cyclotron resonance mass spectrometry (ESI FT-ICR MS): Characterization of complex environmental mixtures. Environ Forensics 2002. doi:10.1080/713848382.

[55] Kim S, Kramer RW, Hatcher PG. Graphical Method for Analysis of Ultrahigh-Resolution Broadband Mass Spectra of Natural Organic Matter , the Van Krevelen Diagram

2003;75:5336–44.

[56] Rivas-Ubach A, Liu Y, Bianchi TS, Tolić N, Jansson C, Paša-Tolić L. Moving beyond the van Krevelen Diagram: A New Stoichiometric Approach for Compound Classification in Organisms. Anal Chem 2018. doi:10.1021/acs.analchem.8b00529.

[57] Prothmann J, Spégel P, Sandahl M, Turner C. Identification of lignin oligomers in Kraft lignin using ultra-high-performance liquid chromatography/high-resolution multiple-stage tandem mass spectrometry (UHPLC/HRMSn). Anal Bioanal Chem 2018;410:7803–14. doi:10.1007/s00216-018-1400-4.

[58] Schmalenberger A, Pritzkow W, Ojeda JJ, Noll M. Characterization of main sulfur source of wood-degrading basidiomycetes by S K-edge X-ray absorption near edge spectroscopy (XANES). Int Biodeterior Biodegrad 2011. doi:10.1016/j.ibiod.2011.08.013.

[59] Cook AM, Laue H, Junker F. Microbial desulfonation. FEMS Microbiol Rev 1998. doi:10.1016/S0168-6445(98)00028-X.

Figure legends

Figure 1. FT-IR analysis of laccase-acetosyringone treated lignin**.**
A) PCA analysis of the normalised absorbance of selected wavelengths at two different incubation time points (0h and 168h). Three different treatments (only lignin, n=2, negative control n=2, and laccase treatment n=6). The arrows represent the component loadings for each variable (wavelength). B) Normalised absorbance in IR spectra of laccase samples before (0h, blue line) and after (168h, red line) incubation with laccase-acetosyringone system.

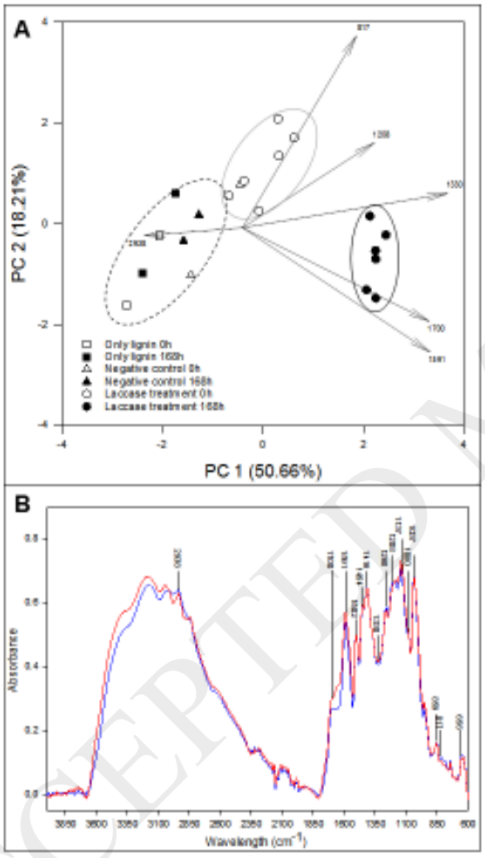

Figure 1

Figure 2 ESI (-) FT-ICR MS spectra of the sample s9-1-0, collected from the laccase-acetosyringone treatment at 0h.
(A) broadband mass spectrum between 100 and 750m/z, (B) 11 peaks of the zoomed in region of 355.00 – 355.30m/z, (C) Van Krevelen diagram, the colour and diameter of the points represent molecular mass (m/z) and relative abundance respectively and (D)% number of compounds present in the commercial lignin product expressed as the mean value (n=3) experimental replicates, laccase treatment at 0h. Lignin O/C:0.3-0.7 and H/C: 1-1.5 (encircled in black); condensed aromatics O/C <0.25 and H/C: 0.5-1.0 (blue); fatty acids or esters/lipids O/C <0.2 and H/C: 1.6-2.0 (yellow); carbohydrates O/C: 0.8 – 1.0 and H/C: 1.65 – 2.0 (green).

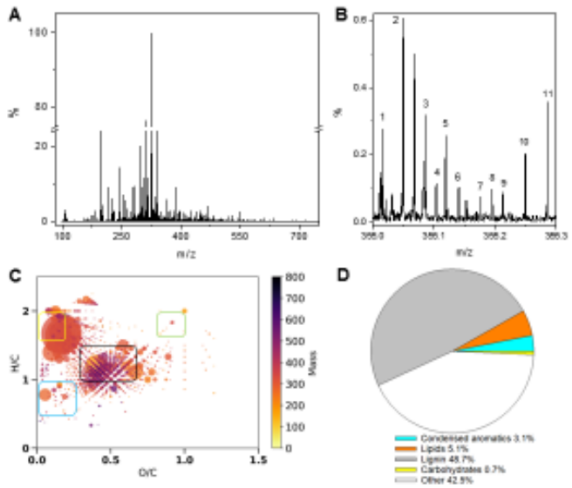

Figure 2

Figure 3. Frequency histograms representing the number of assigned chemical formulae in laccase-acetosyringone treated lignin**.**
(A) Number of total assignments and (B) lignin-type assignments expressed as the mean ± SD (n=3 experimental replicates (white bars), negative control (grey bars) n=2). Columns with different letters indicate significant difference between time points ($p < 0.05$).

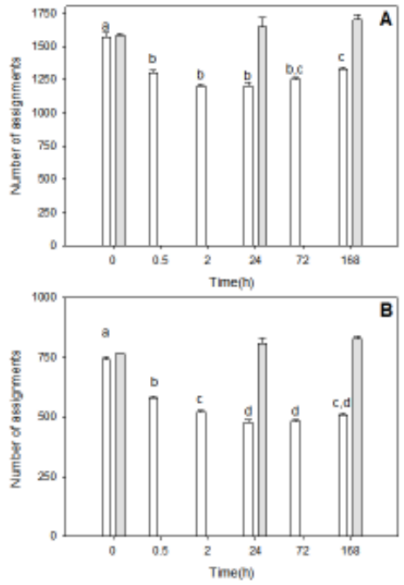

Figure 3

Figure 4. Frequency histograms representing the number of assigned chemical formulae containing sulfur in laccase-acetosyringone treated lignin**.**
(A) Number of total and (B) lignin-type assignments containing S, expressed as the mean ± SD (n=3 experimental replicates (white bars), negative control (grey bars) n=2). Columns with different letters indicate significant difference between time points ($p < 0.05$).

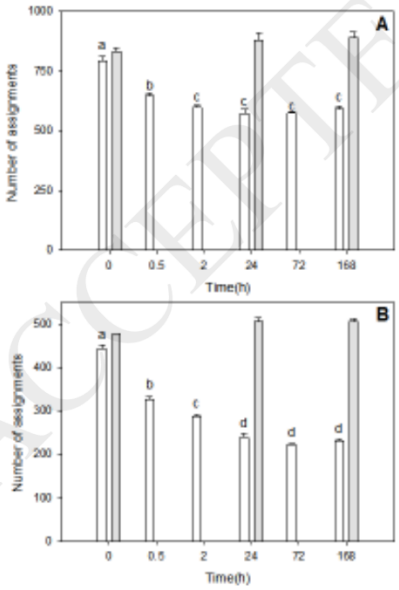

Figure 4

Figure 5. Van Krevelen diagrams to visualise the chemical complexity of lignin before and after treatment with the laccase-acetosyringone.
(A) Van Krevelen diagram of the negative control. (B) Van Krevelen diagram after 24h incubation. A_2 and B_2 show the VK of the lignin region (O/C:0.3-0.7 and H/C: 1-1.5). The colour and diameter of the points represent molecular mass (*m/z*) and relative abundance respectively. The numbers in the arrows indicate the percentage of assignments in common between connected samples.

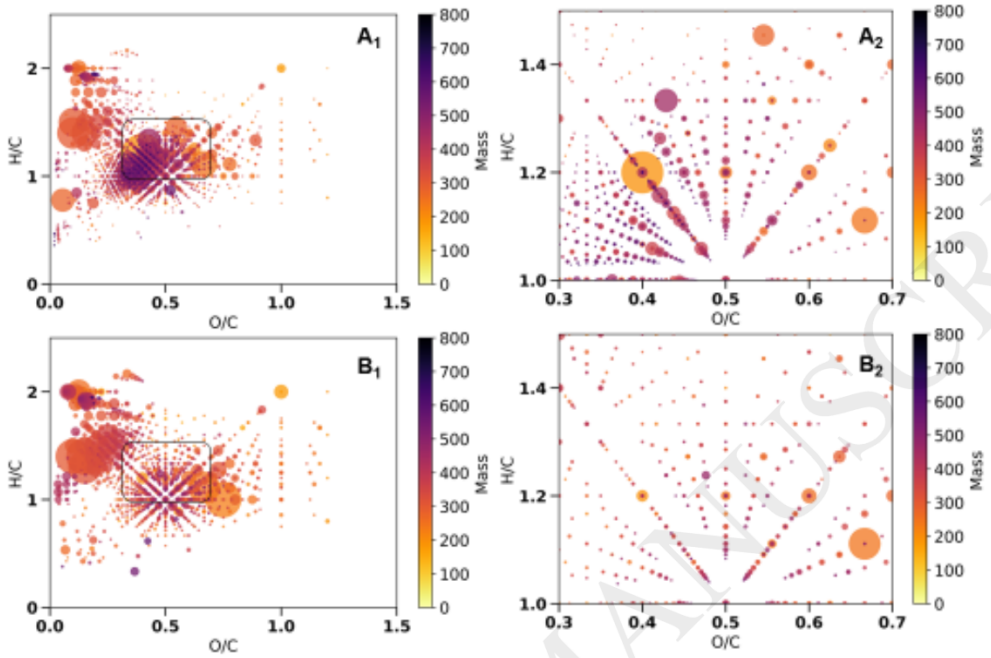

Figure 5

Figure 6. Frequency histograms representing the number of assigned chemical formulae according the m/z**.**
Frequency (counts) of (A) total assignments and (B) lignin-type assignments identified in the laccase treatment (incubation: 0h/ 24h white/black) and in the negative control (0h/ 24h light/dark grey) according to their m/z. Data expressed as the Mean ± SD (n=3, lignin treatment, n=2 negative control)

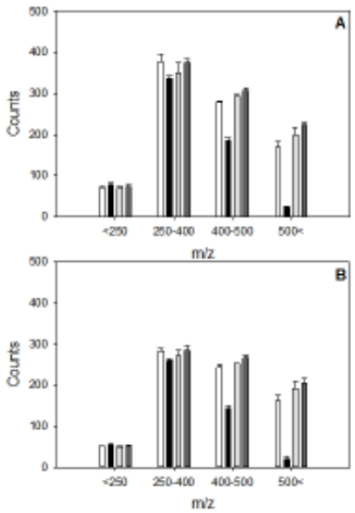

Figure 6

Tables

Table 1 FT-IR band assignment for the lignin polymer used in the present study

Wavelength(cm^{-1})	Bond	Reference
656	sulfonic acid group	[39]
817	C-H out plane vibration guaiacyl unit	[39,41]
859	guaiacyl ring	[39]
1037	aromatic C−H in plane deformation	[39,40]
1080	C−O stretching	[39]
1137	aromatic C-H in plane deformation	[40]
1208	OH plane deformation	[40]
1268	G ring plus C=O stretch	[40]
1330	Phenolic OH; S ring plus G ring condensed	[40]
1416	CH2 scissoring	[40]
1502	aromatic skeletal vibration	[40]
1591	Aromatic skeletal vibrations plus C=O stretch;	[40]
1700	C=O stretch	[40]
2938	symmetric CH2 valence vibration	[40]

Table 2 Component loadings for the wavelengths included in the PCA.

Wavelength (cm^{-1})	PC1	PC2
2938	-0.439	-0.0312
1700	0.835	-0.371
1591	0.839	-0.493
1330	0.917	0.136
1208	0.598	0.337
817	0.509	0.761

Table 3 Exact masses and assigned molecular formulae with associated errors for peaks shown in Figure 2

Number	m/z [M-H]$^-$	Molecular formulae	Error (ppb)
1	355.016309	C11H16O9S2	31
2	355.049312	C15H16O8S1	23
3	355.085715	C16H20O7S1	51
4	355.103462	C16H20O9	17
5	355.118712	C20H20O6	104
6	355.139841	C17H24O8	28
7	355.176227	C18H28O7	84
8	355.194854	C19H32O4S1	59
9	355.212638	C19H32O6	73
10	355.248998	C20H36O5	14
11	355.285383	C21H40O4	11

Table 4 Fragmentation Peaks Observed for the selected sulfur containing compounds.

m/z	Ion formula [M-H]$^-$	Fragmentation	Error (ppm)[a]
439.106502	**$C_{20}H_{23}O_9S$**	M-H	0.740
357.134401	$C_{20}H_{21}O_6$	M-H-SO_3H_2	-0.109
343.118685	$C_{19}H_{19}O_6$	M-H-SO_3H_2 –CH_2	0.078
451.137065	**$C_{21}H_{23}O_9S$**	M-H	0.608
369.134352	$C_{21}H_{21}O_6$	M-H-SO_3H_2	0.027
355.118647	$C_{20}H_{19}O_6$	M-H-SO_3H_2 –CH_2	0.183
455.138127	**$C_{21}H_{27}O_9S$**	M-H	0.418
373.165593	$C_{21}H_{25}O_6$	M-H-SO_3H_2	0.185
359.150014	$C_{20}H_{23}O_5$	M-H-SO_3H_2 –CH_2O	0.412
453.122477	**$C_{21}H_{25}O_9S$**	M-H	0.620
371.149718	$C_{21}H_{23}O_6$	M-H-SO_3H_2	0.792
341.139453	$C_{20}H_{21}O_5$	M-H-SO_3H_2 –CH_2O	-0.017

[a] Mass Spectra were not calibrated post-acquisition which accounts for larger errors.